MINISTRY OF EDUCATION AND TRAINING

VIETNAM ACADEMY OF SCIENCE AND TECHNOLOGY

GRADUATE UNIVERSITY OF SCIENCE AND TECHNOLOGY

Truong Thi Binh Giang

STUDY ON ELECTRODES FABRICATION, STRUCTURAL CHARACTERIZATION, HYPHENATION OF ELECTROCHEMICAL SYSTEMS TO GAS CHROMATOGRAPHY TO ANALYZE THE PRODUCTS OF NITROGEN-CONTAINING COMPOUNDS REDUCTION REACTIONS

SUMMARY OF DISSERTATION ON SCIENCES OF MATTER

Major: Analytical Chemistry

Code: 9 44 01 18

Ha Noi - 2024

The dissertation is completed at: Graduate University of Science and Technology, Vietnam Academy Science and Technology

Supervisors:

1. Supervisor 1: Dr. Duong Tuan Hung - Institute Of Chemistry, Vietnam Academy of Science and Technology

2. Supervisor 2: Dr. Hoang Thi Huong Thao - Institute Of Chemistry, Vietnam Academy of Science and Technology

Referee 1: Assoc.Prof. Dr. Pham Hong Phong

Referee 2: Assoc.Prof. Dr. Pham Tien Duc

Referee 3: Assoc.Prof. Dr.Chu Dinh Binh

The dissertation is examined by Examination Board of Graduate University of Science and Technology, Vietnam Academy of Science and Technology at 09.00 am, December 12th, 2024.

The dissertation can be found at:
1. Graduate University of Science and Technology Library
2. National Library of Vietnam

INTRODUCTION

1. The urgency of the dissertation

Nitrogen compounds and their metabolism play an extremely important role in many aspects of the natural environment in general and of humans in particular. Among them, ammonia (NH_3) is one of the most important chemicals used and produced in the world today. In addition, NH_3 has recently attracted much attention as a chemical that stores hydrogen energy but does not contain carbon, which can be used directly in ammonia fuel cells or indirectly in hydrogen fuel cells. Currently in industry, the synthesis of NH_3 is a huge energy challenge, which mainly relies on the famous Haber-Bosch process.

Based on that problem, the process of converting nitrogen from NO_3^- and N_2 to NH_3 is attracting a lot of research attention from scientists. Among them, the electrochemical method to reduce NO_3^- and N_2 to NH_3 is evaluated by domestic and international scientists as a method with the potential to replace the traditional method.

However, the electrochemical reduction reaction of NO_3^- and N_2 to NH_3 still has two main problems. One is that the conversion efficiency of NO_3^- and N_2 to NH_3 is still low due to slow kinetics and highly competitive side reactions of H_2 gas formation (HER), leading to low reaction activity and poor selectivity. Therefore, the study of effective catalysts that increase the rate of electrochemical reduction of NO_3^- and N_2 to NH_3 is the key to bringing this reaction to industrial scale production, bringing benefits to the environment - energy and socio-economy. However, currently, for the electrochemical reduction reaction of nitrate and nitrogen, electrocatalysts are used with quite low efficiency and selectivity, or quite high cost due to heavy dependence on precious metals. Therefore, the study to find new, more effective catalysts for the electrochemical reduction reaction of nitrate and nitrogen is extremely important. Therefore, in this study, we focused on fabricating Cu-nanosphere with high surface area by a simple electroplating method for the electrochemical reduction of nitrate (NO_3RR) and nitrogen (NRR) to ammonia in an active and selective manner. Notably, Cu-nanosphere exhibited electrocatalytic activity and stability among the best catalysts for NO_3RR and NRR.

Second, the analysis and evaluation of the products formed from the NO_3RR and NRR reactions play an extremely important role in studying these transformation reactions. However, in current publications, this analysis still has many shortcomings, especially the gaseous products of the reaction are often ignored and not analyzed or evaluated.

The analytical method of direct coupling between the chromatographic system and the electrochemical reaction system used in this study will contribute greatly to the direct and accurate determination of the products of the transformation processes, as well as many applications for other reactions. Up to now, the chromatographic-electrochemical coupling system is still quite new, both domestically and internationally. Most electrochemical reduction studies use traditional offline analytical methods. In particular, in Vietnam, the simultaneous or sequential measurement method of reaction products like this has not been studied and developed. Therefore, the study of the chromatographic coupling system for direct analysis of the products of chemical reactions proposed here has high scientific, application and potential significance.

2. Research objectives of the dissertation

- Fabrication, characterization and evaluation of the electrochemical reduction of nitrate and nitrogen by spherical copper nano-electrode (Cu-nanosphere).
- Development of EC-GC coupling system and application to analyze gaseous products of nitrate and nitrogen reduction reaction by electrochemical method.

3. Research content of the dissertation

- Research on the fabrication of Cu-nanosphere electrodes.
- Evaluation of the structural characteristics and electrochemical properties of the electrodes
- Research on coupling gas chromatography with an electrochemical system (EC-GC).
- Development of a method for analyzing N_2 and H_2 gases using an EC-GC system.
- Analysis of the products of the electrochemical reduction of nitrate and nitrogen.
- Evaluation of the catalytic activity of Cu-nanosphere electrodes.

CHAPTER 1. OVERVIEW

Chapter 1 consists of 42 pages, which presents a literature review on nitrate reduction (NO_3RR) and nitrogen reduction (NRR) reactions by electrochemistry, including an overview of the reaction mechanism, some types of electrocatalysts used in NO_3RR and NRR reduction reactions, an overview of the use of Cu electrodes and Cu catalysts in NO_3RR and NRR reduction reactions by electrochemical methods; an overview of research methods and product analysis of nitrate reduction reactions.

CHAPTER 2. RESEARCH METHODS AND EXPERIENCE

Chapter 2, consisting of 20 pages, presents the research methods including Electrode fabrication and structural characterization of electrode materials; establishing the hyphenation of electrochemical system to gas chromatography (EC-GC); developing a method for analyzing products in the gas phase of the electrochemical nitrate reduction reaction and a method for analyzing products of the electrochemical reduction reaction.

CHAPTER 3. RESULTS AND DISCUSSION

3.1. Electrode fabrication and structural characterization of electrode

materials

In this study, Cu-nanosphere was plated by controlling the constant plating current at 4.5 mA/cm^2 for 500 s. In which the plating solution contained Cu^{2+} as the plating ion and 3,5-diamino-1,2,4-triazole (DAT) as the plating process additive.

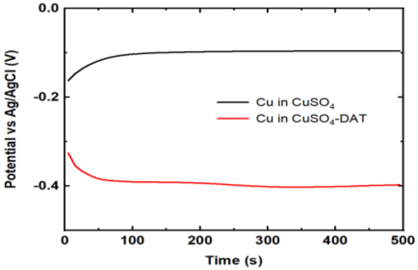

Figure 3.1. Measurement of potential versus time at a density of 4.5 mA/cm^2 of the Cu electrode in 0.1 M CuSO4 solution and in 0.1 M CuSO4 + 10 mM DAT solution.

The SEM and optical images in Figure 3.2 show that the Cu electrode plated in the solution with DAT additive has a spherical particle size of ~ 30 nm. The surface of the Cu electrode with this spherical nanostructure has a matte black color. In contrast, the bare Cu sheet has a smooth, shiny metal surface with a characteristic red-yellow color of copper.
(Figure 3.3).

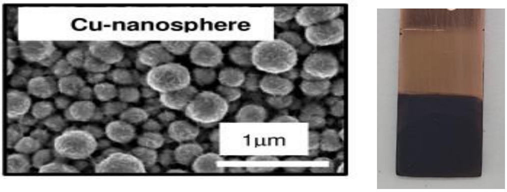

Figure 3.2. SEM image and optical image of Cu electrode with spherical nanoparticle structure (Cu-nanpsphere).

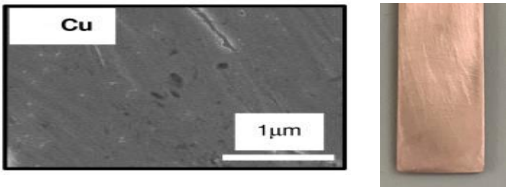

Figure 3.3. SEM image and optical image of Cu electrode.

The XRD patterns of both Cu and Cu-nanosphere (Figure 3.4a) show the characteristic of metallic polycrystalline Cu with Cu (111) peak at 43.29°, Cu(200) peak at 50.43°, and Cu (220) peak at 74.13°. XRD pattern of Cu plate exhibits the dominant appearancesof (111) facet similar to the standard pattern of Cu (JCPDS 00-004-0836).

The XPS spectra of Cu and Cu-nanosphere materials (Figure 3.4b) so confirm the metallic character of both Cu and Cu-nanosphere.

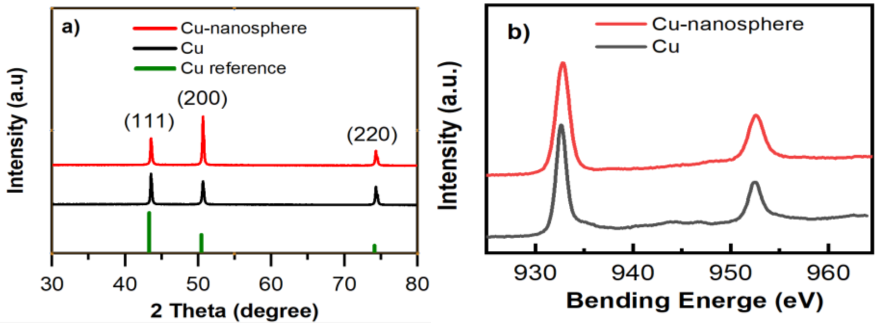

Figure 3.4. a) XRD patterns; and b) XPS patterns of Cu and Cu-nanosphere.

The active surface area of the Cu and Cu-nanosphere electrode were measured by using the Pb underpotential deposition method (Pb UPD) (Figure 3.5). The result shows that the Cu plate exhibits roughness values similar to those from polycrystalline Cu reported before. Alternatively, the Cu-nanosphere electrode exhibits 5.7 times higher active surface area than

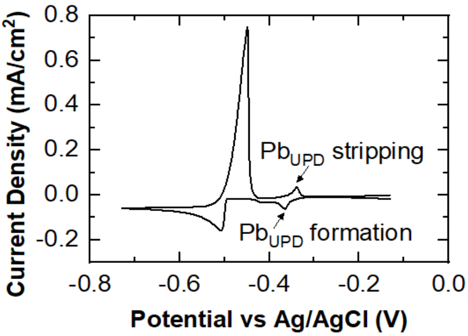

Figure 3.5. CV measurement of Cu-poly in 100 mM $HClO_4$ + 1 mM $Pb(ClO_4)_2$ + 20 mM KCl solution.

the Cu plate (Table 3.1).

Sample	**Pb_{UPD} charge $\mu C/cm^2$**	**$A_{active}/A_{geometric}$**
Cu	453 ± 16	1
Cu-nanosphere	2594 ± 323	5.7

Table 3.1. Pb_{UPD} charge of Cu electrode and Cu-nanosphere.

3.2. Electrochemical characterization of Cu-nanosphere electrode

3.2.1. Linear sweep voltammetry

To evaluate the electrocatalytic activityof Cu-nanosphere for reduction reaction of nitrogenous species,we first conducted electrochemical NO_3RR in a two-compartment H-cell. The anodic and cathodic compartments were separated by a Nafion-117 proton exchange membrane to avoid the oxidation of products at the anode.

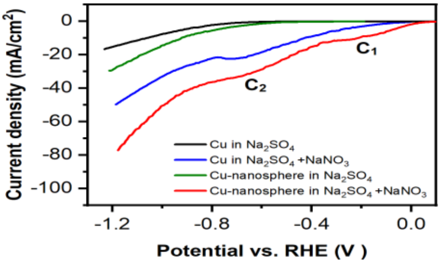

Figure 3.6. LSV in Na_2SO_4 with and without $NaNO_3$ of Cu and Cu-nanosphere.

Figure 3.6 shows LSV curves of Cu and Cu-sphere electrodes in 0.5 M Na_2SO_4 with and without 0.1 M $NaNO_3$ at 10m V/s scan rate. All the reduction current in crease along with the negative shifting of applied potential. The reduction currents in Na_2SO_4 without $NaNO_3$ are associated with water reduction to H_2. The reduction currents in Na_2SO_4 with $NaNO_3$ are associated with NO_3 reduction and H_2 evolution.

Figure 3.6 shows that the Cu and Cu-nanosphere exhibit higher electrochemical activity in electrolyte containing $NaNO_3$ (blue and red line) than in electrolyte without $NaNO_3$ (black and green line).

While the LSV of the electrodes in Na_2SO_4 without $NaNO_3$ shows smooth cathodic sweeps due to the evolution of only one product H_2, the

LSV in Na_2SO_4 with $NaNO_3$ shows wavy peaks at ~ 0.2 V(C_1) and ~ 0.6 V(C_2) due to the formation of different reduction products. It is widely accepted that C_1 represents NO_3^- reduction to NO_2^-, C_2 represents NO_2^- reduction to NH_4^+. Other products are still formed but without clear reduction peaks.

Figure 3.6 also shows that Cu nanosphere exhibits higher electrocatalytic activity than bare Cu. The onset potential of Cu nanosphere is about 0.1 V earlier than that of Cu. The current density of Cu nanosphere is about 1.5 times higher than that of Cu.

3.2.2. Chronoamperometry method

To evaluate the electrochemical nitrate reduction reaction activity, as well as the yield of products during the reduction process, we also performed the reduction reaction at different fixed reduction potentials and measured the current-time on Cu-nanosphere and Cu electrodes in Na_2SO_4 + $NaNO_3$ electrolyte.

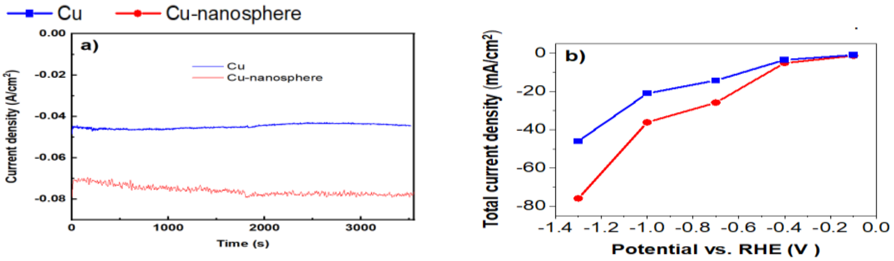

Figure 3.7. a) CA measurement of Cu electrode and Cu-nanosphere in 0.5 M Na_2SO_4 + 0.1 M $NaNO_3$ solution at reduction potential -1.3 V vs. RHE; b) Total reduction current at corresponding potentials of Cu electrode and Cu-nanosphare.

Figure 3.7 shows the current density curves of Cu electrode and Cu-nanosphere versus time at -1.3V vs. RHE in 0.5M Na_2SO_4 + 0.1M $NaNO_3$ solution. From the reduction current densities obtained at different reduction potentials, the average reduction current density at each reduction potential of the reduction reaction is calculated and shown in Figure 3.7b. Figure 3.7b shows that Cu-nanosphere exhibits higher reduction current density than Cu at all potentials.

3.3. Gas chromatography coupled to electrochemical reaction system

3.3.1. Automatic gas sampler

To solve the airtight problem, we set up an online automatic gas sampling method on a continuous gas stream in this study. In which the gas source (gas cylinder or gas generating reactor) is directly connected to the inlet of the GC system. To control the fixed amount of gas for GC analysis, in this study, we chose to pair an automatic sampler on a continuous gas stream, including a gas flow controller, a sample loop, and a 6-port valve.

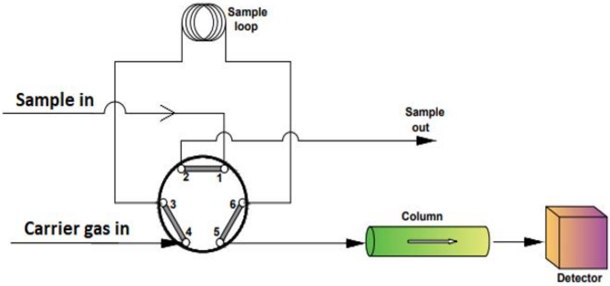

Figure 3.8. Schematic diagram of the sampler in the closed valve position.

3.3.2. Gas phase sample system for developing analytical methods

It is extremely important to set up a series of gas samples with different concentrations to investigate and develop a process for analyzing gas products of electrochemical reactions. Therefore, in this study, we have established a gas sample phase system to dilute high concentration standard gas samples to any desired concentration by coupling two mass flow controllers (Mass Flow Controller – MFC).

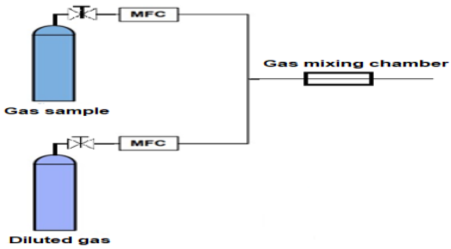

Figure 3.9. Diagram of gas phase system.

To evaluate the reliability of the gas phase system established in this study, the 2.0% H_2 gas sample was prepared from 0.2 sccm of 100% H_2 gas and 9.8 sccm of 100% He gas, and the H_2 gas sample from the 2% H_2 standard gas cylinder was analyzed 6 times. The repeatability of the gas phase system was evaluated by the relative standard deviation (RSD) value compared to the AOAC acceptance threshold. The accuracy of the gas phase system was evaluated by the similarity of the gas phase system and the standard gas cylinder by comparing the 2 variances using the F–Fisher standard and comparing the average values between the 2 types of gas using the Student's t-standard.

Table 3.2. GC peak area results of replicate analyses of 2.0% H_2 gas samples from the gas phase system and from the standard gas cylinder.

Numerical order	**Peak area of H_2 2,0% from gas phase system H_2 with He**	**H_2 2,0% peak area from standard gas cylinder**
Medium	0.1191	0.1201
Standard Deviation SD	0.0023	0,0012
Relative standard deviation RSD %	1.8935	1.0045
Variance S^2	$5.083.10^{-6}$	$1.455.10^{-6}$
F experimental F_{tn}	3.494	
F_c(0.05; 5.5)	5.050	
Common standard deviation S_c^2	$3.269.10^{-6}$	
t experimental t_{tn}	0.875	
t(0.05;10)	2.228	

The evaluation results show that the gas preparation method using this study's gas phase system is reliable for developing analytical methods.

3.3.3. EC-GC coupling system

To analyze the gas products of the nitrate reduction reaction, the product gases need to be removed from the reaction system and introduced into the analysis system accurately and stably. Therefore, in this study, we set up an analysis system in which the product gases generated from the electrochemical reaction from the cathode chamber in the H-shaped reaction vessel follow the He gas stream out of the reaction vessel. The gas stream, after leaving the reaction vessel, is passed through a column containing silica gel crystals to retain the water vapor that may arise from the reaction vessel so that the gas entering the GC column must be dry gas, avoiding affecting the durability of the GC column and affecting the measurement.

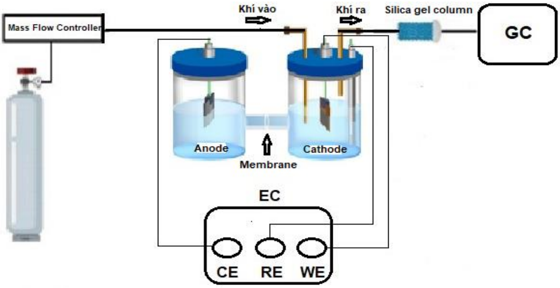

Figure 3.10. Diagram of the coupling system between the electrochemical reaction and the gas chromatography system.

3.4. Electrochemical nitrate reduction reaction

3.4.1. Method development and validation of H_2, N_2 gas analysis method

3.4.1.1. H_2 gas analysis

a. Survey of H_2 analysis conditions

Figure 3.11 is the chromatogram of H_2 gas; in which the first negative peak is the peak of H_2, the next peaks are O_2 and N_2 from the atmosphere, respectively, which cannot be removed during the analysis.

Column pressure and temperature greatly influence the retention time, sensitivity, resolution and peak width of the analyte.

Therefore, we simultaneously investigated the two factors of pressure and column temperature to optimize three indexes, including peak area, retention time, and resolution R. The pressure factor was investigated at the conditions of 1.0 – 4.0 psi. The temperature factor was investigated at the conditions of 30°C - 50°C. The sample was a 4.762% H_2 gas sample mixed from 0.5 sccm of 100% H_2 gas and 10 sccm of 100% He gas.

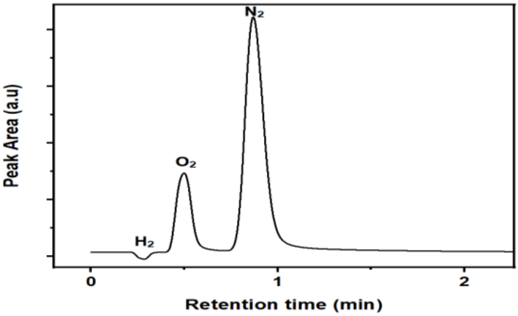

Figure 3.11. Chromatogram of H_2 gas.

Based on the above survey results, we choose the pressure conditions of 3.0 psi and 30°C to continue to build the H_2 analysis process for the nitrate reduction reaction. In other reaction applications, when the product gas mixture includes many other gases, the H_2 analysis conditions can be considered and reselected to suit the analysis conditions of the new gas mixture.

b. Determine the linear range and construct the standard curve of the H_2 analysis method

Figure 3.12.a is the GC chromatogram of H_2 gas at different concentrations, showing that the GC signal is proportional to the H_2 gas concentration. The correlation between the concentration and the GC peak area of H_2 gas is shown in Figure 3.12a and Figure 3.12.b. The results show that the linear range of the H_2 analysis method by GC is 0 – 1.961%.

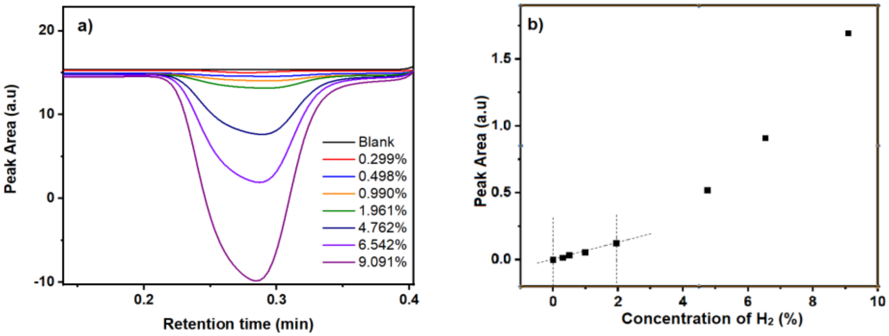

Figure 3.12. a) GC chromatograms of H_2 gas at different concentrations, b) Investigation of the linear range of the H_2 analysis method.

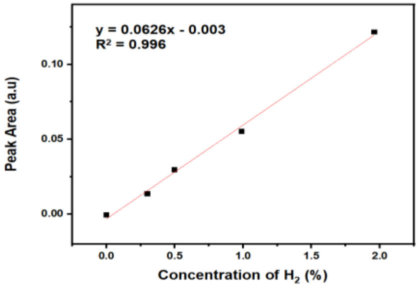

Figure 3.13. Linear calibration curve of H_2 gas.

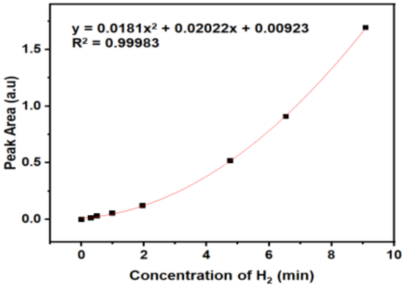

Figure 3.14. Quadratic calibration curve of H_2 gas.

Measurement of H_2 concentration by gas chromatography sometimes results in a calibration curve that is quadratic rather than linear. This can occur due to a number of factors. Thermal conductivity detectors (TCDs) used in gas chromatography measure the thermal conductivity of gas mixtures. The relationship between hydrogen concentration and thermal conductivity is not always linear, especially at high concentrations.

Thus, using the quadratic calibration curve in gas chromatography helps to increase the accuracy and reliability of hydrogen gas concentration measurement, ensuring that the analytical results reflect the actual relationship between analyte concentration and detector signal.

c. Determination of MDL and MQL values of H_2 gas analysis method

Table 3.3. Detection limit (MDL) and quantification limit (MQL) of H_2 gas analysis method.

Numerical order	**H_2 concentration calculated according to the linear calibration curve (%)**	**H_2 concentration calculated according to the quadratic calibration curve (%)**
Average concentration (%)	0.5068	0.6210
Standard Deviation SD	0.0074	0.0108
MDL (%)	0.022	0.0325
MQL (%)	0.067	0.0975

The experimental results show that both standard curves give low MDL and MQL values, proving that the method and both regressions are reliable and have high sensitivity.

d. Accuracy of H_2 analysis method

- Determination of precision of H_2 analysis method

Table 3.4. Results of replicate analyses of H_2 samples 0.498, 1.961, and 9.091%.

Sample H_2 (%)	**0.498**		**1.961**		**9.091**	
	Linear	**Quadratic**	**Linear**	**Quadratic**	**Linear**	**Quadratic**
Average concentration (%)	0.504	0.61674	1.973	1.98356	26.70	9.032
Standard Deviation SD	0.00378	0.00556	0.01109	0.00755	0.5009	0.09071
RSD (%)	0.751	0.902	0.5621	0.381	1.876	1.004

From the above results, we can conclude that for the first-order standard curve of H_2, the precision meets the requirements for analyzing samples with low concentrations in the range of 0 – 1.961%. As for the second-order standard curve, the precision is guaranteed for all samples with concentrations from 0 – 9.091%. This conclusion is very important in choosing the appropriate standard curve for each sample with different concentrations when performing subsequent measurements.

- Determining the accuracy of the H_2 analysis method

Table 3.5. Recovery results of sample of H_2 gas 2.0%.

Numerical order	**H_2 concentration calculated by linear calibration curve**	**H_2 concentration calculated by quadratic calibration curve**
Average concentration (%)	1.973	1.984
Recovery (R%)	98.63	99.18

The results show that the H_2 analysis method just built with both regression equations has the required accuracy. Thus, the H_2 content analysis process by GC method has high accuracy, good repeatability and can be applied to analyze H_2 content in gas samples. The first-order regression equation is suitable for H_2 concentration from 0 – 2.0%, the second-order linear regression equation is suitable for H_2 concentration up to 10%.

3.4.1.2. N_2 gas analysis

a. Survey of N_2 analysis conditions

The survey results show that N_2 is an easy-to-analyze gas, and good analysis efficiency can be achieved under many different analysis conditions. Therefore, when analyzing N_2 in a mixture of other gases to be analyzed, the analysis conditions can be selected according to the priority of other gases to be analyzed. Based on the above survey results, we choose the pressure conditions of 3.0 psi and 30°C to continue to build the N_2 analysis process for the nitrate reduction reaction.

b. Determine the linear range and build the calibration curve of the N_2 gas analysis method

- Determine the linear range of the N_2 gas analysis method

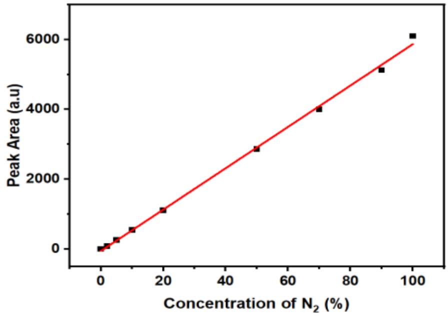

Figure 3.15. Linear range of N_2 gas analysis method.

From Figure 3.15, we can see that the N_2 gas analysis method has a linear concentration range from 0 – 100%.

Based on the practical need to serve product analysis because N_2 is produced from nitrate reduction reaction with a small amount of product gas, we proceed to build a standard curve of N_2 gas at a small concentration. The standard curve is built on a series of N_2 gas with a concentration range of 0, 2, 5, 10, and 20%.

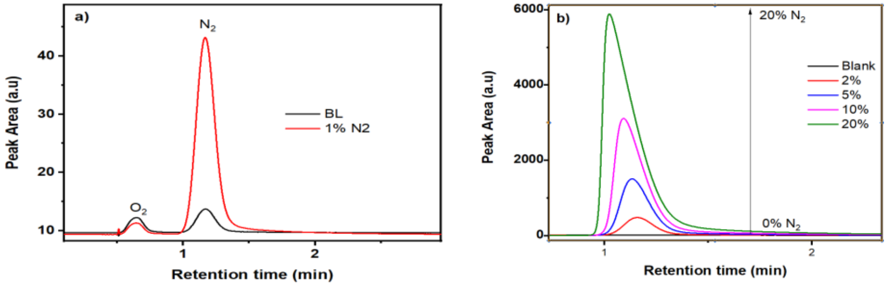

Figure 3.16. a) GC chromatogram analyzing N_2 gas from air in blank sample and from 1% N_2 gas sample; b) N_2 gas spectrum from concentration 0 – 20%.

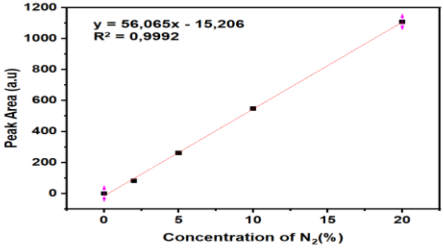

Figure 3.17. Standard curve N_2 after direct background subtraction of sample N_2 peak = measured N_2 peak – background N_2 peak.

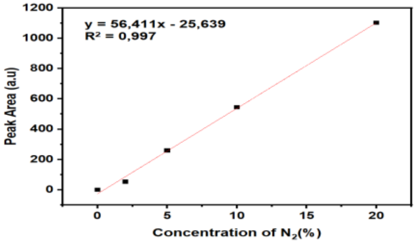

Figure 3.18. N_2 standard curve minus background at N_2 ratio.

c. Determination of MDL and MQL values of N_2 gas analysis method

Table 3.6. Detection limit (MDL) and quantification limit (MQL) of N_2 gas analysis method.

Numerical order	**N_2 concentration calculated from the background subtraction standard curve**	**N_2 concentration calculated from the standard curve minus the background according to the N_2/O_2 ratio**
Average concentration (%)	0.2941	0.477
Standard Deviation SD	0.1978	0.00085
MDL (%)	0.5935	0.0026
MQL (%)	1.780	0.0077
Recovery (%)	**58.82**	**95.40**

The experimental results show that: MDL, MQL calculated when using the direct background subtraction N_2 standard curve have much higher values than MDL, MQL values when using the background subtraction standard curve according to the N_2/O_2 ratio. Furthermore, from the results of N_2 recovery calculated from the two standard curves, it shows that the recovery calculated by the background subtraction standard curve according to the N_2/O_2 ratio gives the result H = 95.40%, ensuring according to AOAC standards, while the N_2 recovery by the background subtraction standard curve gives the result low. From the results of MDL, MQL determination and the above reasons, we agree to use the N_2 standard curve minus the background according to the N_2/O_2 ratio for real sample analysis of nitrate reduction reaction.

d. Determination of the accuracy of the N_2 analysis method

- Determination of the precision of the N_2 analysis method

Table 3.7. Results of replicate analysis of the N_2 sample 0.5%; 10% and 20%.

Sample N_2	**0.5%**	**10%**	**20%**
Average concentration (%)	0.4771	10.194	20.142
Standard Deviation SD	0.00088	0.00440	0.00992
RSD (%)	0.18	0.0431	0.0493

Comparing this calculated value with the expected value according to AOAC shows that the N_2 analytical method has satisfactory precision.

- Determining the accuracy of the N_2 analytical method

Table 3.8. Recovery results of N_2 gas samples 0.5%; 10% and 20%.

Sample N_2	**0.5%**	**10%**	**20%**
Average concentration (%)	0.4771	10.194	20.142
Recovery R (%)	**95.43**	**101.94**	**100.71**

Comparing this calculated value with the desired value according to AOAC shows that the N_2 analysis method just developed has the required accuracy. Thus, the N_2 content analysis process using the GC method investigated and developed above has high accuracy, good repeatability and can be applied to analyze N_2 content in gas samples.

3.4.2. Analysis of the products of the electrochemical nitrate reduction reaction

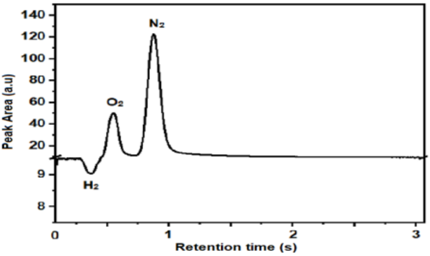

Figure 3.19. Chromatogram of H_2 and N_2 gas products of the electrochemical nitrate reduction reaction using Cu-nanosphere electrode at -1.3V vs. RHE.

Table 3.9. Total yield of electrochemical nitrate reduction products.

	Cathode potential (V vs RHE)	**Faradaic efficiency of H_2 (%)**	**Faradaic efficiency of N_2 (%)**	**Faradaic efficiency of NH_4^+ (%)**	**Faradaic efficiency of NO_2^- (%)**	**Total Faradaic efficiency (%)**
Cu	**-0.1**	0	0	2.94	90.75	**93.69**
	-0.4	0	12.41	14.48	84.99	**111.88**
	-0.7	7.83	1.15	54.60	26.77	**90.35**
	-1.0	9.85	0.11	64.35	19.94	**94.25**
	-1.3	11.98	1.34	74.80	8.358	**96.48**
Cu-nanosphere	**-0.1**	0	0	3.790	92.08	**95.87**
	-0.4	0	0	12.94	86.71	**99.65**
	-0.7	3.87	2.94	40.04	58.38	**105.23**

	-1.0	7.05	5.23	68.28	18.54	**99.10**
	-1.3	4.47	2.72	85.63	10.38	**103.20**

Using the analytical procedures developed in this study, the products including H_2, N_2, NH_4^+ and NO_2^- were found to be specific for each condition of the nitrate reduction reaction. The total Faradaic efficiency of all products was 93.7 – 105.2%. This is a relatively good result under the reaction and analysis conditions with many influencing factors that can cause losses. This result shows that the developed methods have met the requirements for almost completely analyzing the products of the nitrate electrochemical reduction reaction.

3.4.3. Evaluation of NH_4^+ synthesis efficiency and rate of electrochemical nitrate reduction reaction

Among the products of nitrate reduction reaction, ammonium product is being studied the most due to its potential application and economic and environmental efficiency. To evaluate the efficiency of NH_4^+ synthesis in the NO_3RR process, we analyzed the NH_4^+ content formed, and then calculated the efficiency and rate of NH_4^+ synthesis of nitrate reduction reaction on Cu-nanosphere and Cu electrodes.

Figure 3.20a shows that the NH_4^+ FE of Cu and Cu-nanosphere increases with the potential being more negative. The NH_4^+ FE of Cu starts from ~ 3% at -0.1 V and reaches ~ 75% at -1.3 V NH_4^+; the NH_4^+ FE Cu-nanosphere starts from ~ 4% at -0.1 V and reach ~85% at -1.3 V NH_4^+.

Figure 3.20b shows that NO_3RR to form NH_4^+ occurs at all potentials above -0.1 V. While the NH_4^+ FE of Cu and Cu-nanosphere are somewhat similar, the NH_3 yield of Cu nanosphere is higher than of Cu. At -1.3 V, the NH_4^+ yield of Cu-nanosphere reaches 5.2 mg/h.cm^2, which is ~ 2 times higher than of Cu. This data suggests that electrocatalytic activity for NO_3RR of Cu-nanosphere is higher than that of Cu electrode.

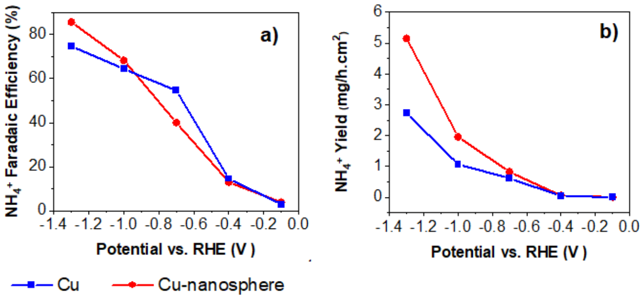

Figure 3.20. a) Faradaic efficiency (FE) of NH_4^+ formation; b) NH_4^+ yield rate of Cu-nanosphere of NO_3RR at -1.3 V in 0.5 M Na_2SO_4 + 0.1 M $NaNO_3$ solution.

To evaluate the durability of Cu-nanosphere, CA tests are performed at -1.3 V for 10 consecutive cycles. Figure 3.21 shows that the Cu-nanosphere exhibits excellent stability with NH_4^+ yield rate and FE remains almost the same after 10 cycles (~98% performance retention). This high stability for NO_3RR of Cu-nanosphere film could originate from its fabrication method. Cu-nanosphere was fabricated by electroplating on Cu electrode.

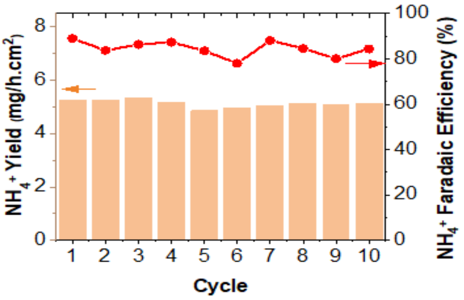

Figure 3.21. Stability test of Cu nanosphere of NO_3RR at -1.3 V in 0.5 M Na_2SO_4 + 0.1 M $NaNO_3$ solution.

^{15}N isotope labeling experiments were conducted to confirm that the ammonium detected in the NO_3RR experiment was indeed derived from nitrate. This result confirmed that the ammonia formation originated from the electroreduction of nitrate and ruled out contamination from N_2 gas, chemicals, laboratory environment, and catalyst.

$Na^{15}NO_3$ (99% atomic mass) was used as the reactant to perform NO_3RR isotope experiments to clarify the origin of the produced ammonia. ^1H-NMR was performed at 25°C on a Bruker Ascend 600 MHz using DMSO-d6 solvent.

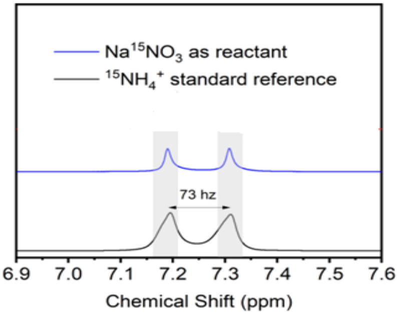

Figure 3.22. ^{1}H-NMR spectrum (600 MHz, DMSO-d6) of $^{15}NH_4^+$ produced from NO_3RR using $Na^{15}NO_3$ as reactant.

3.5. Electrochemical nitrogen reduction reaction

3.5.1. Electrocatalytic activity for NRR of Cu-nanosphere

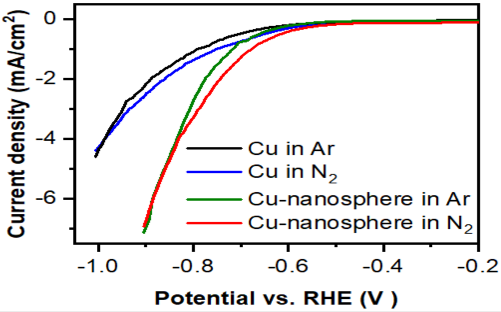

Figure 3.23. LSV in Ar and N_2 saturated environment in Na_2SO_4 of Cu electrode and Cu-nanosphere.

Figure 3.23 also shows that the Cu and Cu-nanosphere exhibit higher current density in N_2-saturated environment than in Ar. The significant difference in the LSV curves of N_2 and Ar is found at the potential from -0.4 V to -0.8 V.

3.5.2. Evaluation of NH_4^+ efficiency and yield rate during electrochemical nitrogen reduction reaction

Figure 3.24.a shows that the Cu-nano sphere exhibitsa higher reduction current density than the Cu at potential steps from -0.4 V to -0.8V, especially at -0.7 V and -0.8 V. This reduction current from the CA is consistent with the one from the LSV described above (Figure 3.23).

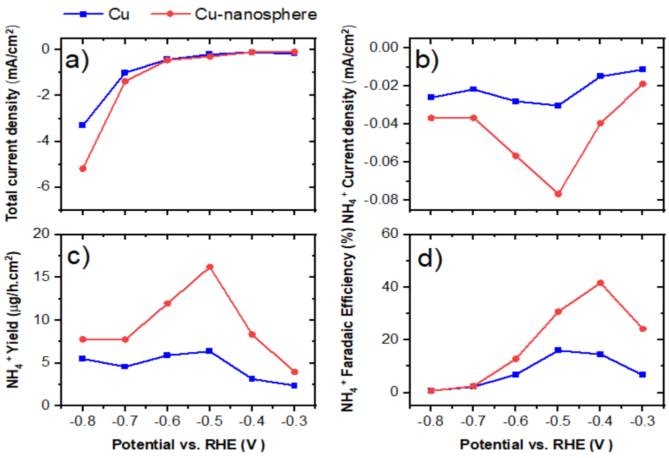

Figure 3.24. a) Total reduction current at corresponding potentials, b) Partial current density, c) Yield rate, and d) Faradaic efficiency of NH_4^+ formation from NRR in N_2-saturated 0.5 M Na_2SO_4.

Figure 3.24.b and 3.24.c show that both the absolute value of partial current density and the yield rate of NH_4^+ formation is larger than 0 at all potential steps from -0.3 V to -0.8 V. Figure 3.24.d shows that the NH_4^+ FE of Cu and Cu-nanosphere increases with the potential being more negative. While the NH_4^+ FE of Cu reaches a maximum value of 16.0% at -0.5 V, the FE of Cu-nanosphere reaches a maximum value of 41.6% at a smaller potential of -0.4 V. At more negative potential, the NH_4^+ FE of both Cu and Cu-nanosphere decreases considerably and reaches ~0.7% at -0.8 V, which suggests that HER is the dominant reaction at the cathode. When the HER being dominant, most electrons and protons go toward reducing H_2O to H_2 instead of reducing N_2 to ammonia, resulting in low NH_4^+ FE.

Evaluation of the durability of the action

To evaluate the durability of the Cu-nanosphere, chronoamperometry tests are performed on the potential of maximum FE -0.4 V for 10 consecutive cycles. Figure 3.25.b shows that the Cu nanosphere exhibits excellent stability with small decreases in NH_4^+ yield rate (~85% performance retention), but the FE remains somewhat the same after 5 cycles. This high stability for NRR of Cu-nanosphere film could originate from the self-supported structure of the electrodeposited Cu-nanosphere, as explained above. XRD and XPS pattern (Figure 3.25.c, 3.25.d) show that Cu-nanosphere retains the metallic property and (200) facet dominance after the electrolysis experiments. This data suggests that the Cu-nanosphere film is stable on the electrode even after vigorous bubbling gas and product evolution of the electrolysis.

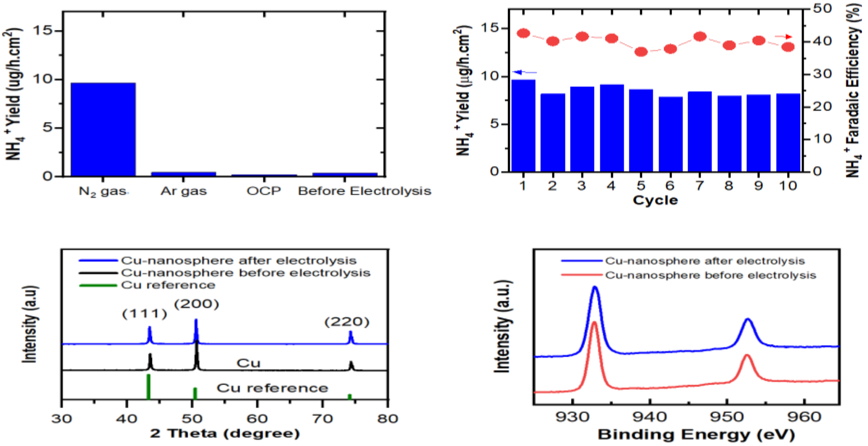

Figure 3.25. a) NH_4^+ yield rate of Cu-nanosphere in N_2 environment, Ar environ ment, at OCP with no electrolysis, and before the electrolysis; b) Stability test of NRR on Cu-nanosphere at -0.4 V for 10 consecutive cycles; c) XRD patterns; and d) XPS patterns of Cu-nanosphere before and after electrolysis.

^{15}N isotope labeling experiments were conducted to confirm that the ammonium detected in the NRR experiments was indeed derived from nitrogen. This result confirmed that the ammonium formation was due to electrolytic denitrification and ruled out contamination from other sources.

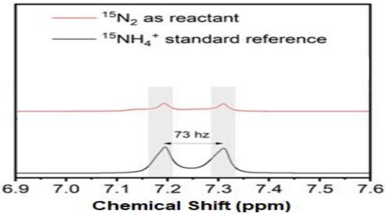

Figure 3.26. ^1H-NMR spectrum (600 MHz, DMSO-d6) of $^{15}NH_4^+$ produced from NRR using $^{15}N_2$ as reactant.

CONCLUSIONS

With the aim of studying the development of a direct coupling system between electrochemistry and gas chromatography in the analysis of products from the nitrate reduction reaction and evaluating the catalytic activity of working electrodes Cu and Cu-nanosphere, the dissertation has achieved the following results:

1. A Cu-nanosphere electrode with a large electrochemical active area has been fabricated by electroplating in the presence of DAT plating additives. The Cu-nanosphere electrode shows superior catalytic activity for nitrate and nitrogen reduction reactions compared to conventional Cu electrodes.

2. A successful direct coupling of the nitrate reduction electrochemical reaction system with GC gas chromatography has been studied to analyze gas products.

3. The optimal conditions have been studied, surveyed, and evaluated, and the reliability of the H_2 and N_2 gas analysis methods has been evaluated. The analysis method has high reliability, meeting the requirements for analyzing the content of H_2 and N_2 gases within the concentration range that the method has been developed.

4. All products of the nitrate reduction reaction, including gaseous products H_2, N_2, and liquid products (NH_4^+, NO_2^-), were evaluated from the developed method. The total yield of all products of nitrate reduction reaction ≈ 100%. That means we have evaluated all products of nitrate reduction reaction through the developed method.

5. Cu-nanosphere catalyst electrode was applied to study nitrogen reduction reaction by electrochemical method. This reaction has also contributed to expanding the analysis objects in the study of Cu-nanosphere catalyst electrode.

NEW CONTRIBUTIONS OF THE DISSERTATION

1. Nanostructured Cu-nanosphere electrodes were fabricated by electroplating in the presence of a DAT plating additive. Compared to conventional Cu electrodes, the Cu-nanosphere electrodes exhibited superior catalytic activity for nitrate and nitrogen reduction reactions and high efficiency and selectivity for NH_4^+ synthesis.

2. For the first time, the EC-GC coupling system was successfully built and the parameters were optimized for application in the analysis of gas products of chemical reactions. The EC-GC coupling system was applied to optimize and confirm the usability of the gas product analysis process, and modern analytical methods were combined to analyze all the main products of the nitrate electrochemical reduction reaction.

LIST OF PUBLICATIONS

1. Hoang Thi Huong Thao, **Truong Thi Binh Giang**, Nguyen Thi Ngoc Bich, Duong Tuan Hung, Vu Duc Loi, 2021, Synthesis of CuFe on oriented Cu electrode as a highly active catalyst for nitrate reduction reaction by electrochemical method, *Volume B of Vietnam Journal of Science and Technology*,63(11DB),pp.60-65. https://doi.org/10.31276/VJST.63(11DB).60-65.
2. **Truong Thi Binh Giang**, Nguyen Thi Ngoc Bich, Duong Tuan Hung, Vu Duc Loi, Hoang Thi Huong Thao, 2021, Online determination of N2 and H2 products of the electrochemical nitrate reduction reaction by gas chromatography with thermal conductivity detector TCD, *Journal of Analytical Chemistry, Physics and Biology*, 26(2), pp. 61-66.
3. **Truong Thi Binh Giang**, Vu Duc Loi, Duong Tuan Hung, Hoang Thi Huong Thao, 2022, Determination of nitrate reduction reaction products on Cu catalyst by UV-VIS spectroscopy and online Gas Chromatography, *The 7th analytica Vietnam Conference, Vietnam National University Press, Hanoi, Ho Chi Minh City*, pp. 303-311.
4. **Giang Binh Truong**, Hung Tuan Duong, Loi Duc Vu, Thao Thi Huong Hoang, 2023, Highly Efficient Electrochemical Nitrate and Nitrogen Reduction to Ammonia under Ambient Conditions on Electrodeposited Cu-Nanosphere Electrode, *European Journal of Inorganic Chemistry*, 26(31), p e202300371. https://doi.org/10.1002/ejic.202300371.
5. **Truong Thi Binh Giang**, Duong Tuan Hung, Vu Duc Loi, Hoang Thi Huong Thao, 2023, Determination of products of electrochemical nitrate reduction reaction on Cu catalyst by UV-Vis absorption spectroscopy and online gas chromatography, *Volume B of Vietnam Journal of Science and Technology*, 65(8), pp. 45-49. https://doi.org/10.31276/VJST.65(8).45-49.